

See discussions, stats, and author profiles for this publication at: <https://www.researchgate.net/publication/234169207>

PHEMA-Based Thin Hydrogel Films for Biomedical Applications.

Article in *Journal of Bioactive and Compatible Polymers* · July 2011

DOI: 10.1177/0883911511410460

CITATIONS

40

READS

2,108

6 authors, including:



Elvira De Giglio

University of Bari Aldo Moro

150 PUBLICATIONS 4,375 CITATIONS

[SEE PROFILE](#)



Marco Domingos

The University of Manchester

79 PUBLICATIONS 3,649 CITATIONS

[SEE PROFILE](#)



Monica Mattioli-Belmonte

Marche Polytechnic University

259 PUBLICATIONS 7,830 CITATIONS

[SEE PROFILE](#)



Stefania Cometa

Jaber innovation s.r.l.

112 PUBLICATIONS 3,102 CITATIONS

[SEE PROFILE](#)

Journal of Bioactive and Compatible Polymers

<http://jbc.sagepub.com/>

PHEMA-based thin hydrogel films for biomedical applications

E De Giglio, D Cafagna, M M Giangregorio, M Domingos, M Mattioli-Belmonte and S. Cometa

Journal of Bioactive and Compatible Polymers published online 17 June 2011

DOI: 10.1177/0883911511410460

The online version of this article can be found at:

<http://jbc.sagepub.com/content/early/2011/06/17/0883911511410460>

Published by:



<http://www.sagepublications.com>

Additional services and information for *Journal of Bioactive and Compatible Polymers* can be found at:

Email Alerts: <http://jbc.sagepub.com/cgi/alerts>

Subscriptions: <http://jbc.sagepub.com/subscriptions>

Reprints: <http://www.sagepub.com/journalsReprints.nav>

Permissions: <http://www.sagepub.com/journalsPermissions.nav>

PHEMA-based thin hydrogel films for biomedical applications

Journal of Bioactive and
 Compatible Polymers
 0(0) 1–15

© The Author(s) 2011

Reprints and permissions:

sagepub.co.uk/journalsPermissions.nav

DOI: 10.1177/0883911511410460

jbc.sagepub.com



**E De Giglio¹, D Cafagna¹, MM Giangregorio¹,
 M Domingos², M Mattioli-Belmonte³ and S Cometa⁴**

Abstract

Poly(2-hydroxyethyl methacrylate) based thin coatings were electro-synthesized by cyclic voltammetry on Au-coated quartz crystal surfaces to study different solid–liquid interfacial processes. By varying the electrochemical parameters and the presence or not of a crosslinking agent, films were obtained with thicknesses ranging from 5 to 90 nm. Surface characterization was performed by X-ray photoelectron spectroscopy, atomic force microscopy, and static contact angle measurements. Using quartz crystal microbalance with dissipation monitoring to investigate the relationship between the film thickness and the swelling behavior, it was found that these characteristics can be modulated by varying either the number of voltammetric cycles or the presence of the crosslinker. Cell adhesion and biocompatibility tests indicate that these film coatings were suitable for biomedical applications.

Keywords

PHEMA-based thin films, electro-synthesis, film swelling, fibroblasts, QCM-D

Introduction

In the biomedical field, the capability to reproduce the micro and/or nano-scale textured surfaces to improve cell viability remains a major challenge. Due to their structural similarity to natural tissues, hydrogels are gaining interest as carrier systems for the controlled release and delivery of therapeutic agents.¹ The optimal performances of hydrogels in biological environments are especially related to their capability to retain large amounts of water.²

¹Department of Chemistry, University of Bari 'Aldo Moro', Bari, Italy

²Centre for Rapid and Sustainable Product Development, Polytechnic Institute of Leiria (IPL), Leiria, Portugal

³Department of Molecular Pathology and Innovative Therapies, Università Politecnica delle Marche, Ancona, Italy

⁴Laboratory of Bioactive Polymeric Materials for Biomedical & Environmental Applications, Department of Chemistry and Industrial Chemistry, University of Pisa, Pisa, Italy

Corresponding author:

S. Cometa, Laboratory of Bioactive Polymeric Materials for Biomedical & Environmental Applications, Department of Chemistry and Industrial Chemistry, University of Pisa, Pisa, Italy

Email: cometa@ns.dcci.unipi.it

Poly(2-hydroxyethyl methacrylate) (PHEMA) was the first synthetic hydrogel used in the medical and pharmaceutical fields. For example, PHEMA and PHEMA-based hydrogels applications are used as controlled drug release systems, including protein release,^{3–5} breast augmentation surgery,⁶ synthetic skin⁷ and employed in the development of contact lenses by Wichterle and Lim.⁸ Recently, photopolymerization of PHEMA-based hydrogels were investigated to create three-dimensional scaffolds for soft tissue engineering.^{9,10} Researchers from the Centre for Rapid and Sustainable Product Development of the Polytechnic Institute of Leiria (Portugal) are developing a new stereolithographic fabrication process named micro stereo-thermal-lithographic process to produce multimaterial functionally graded scaffolds.¹¹ This process uses ultraviolet radiation and thermal energy (infrared radiation) to initiate the polymerization reaction in a medium containing both photo- and thermal-initiators. Three-dimensional PHEMA scaffolds were successfully produced using the direct mask-based writing system.¹⁰

PHEMA is a moderately swellable polymer system; the swelling equilibrium degree depends both on the polymerization mechanism and crosslinker (presence or not, the amount and chemical nature).^{12–15} In the case of hydrogel membranes and/or films, the thickness of the films is another factor that affects water uptake—thin films present different behaviors compared to thick films.¹⁶ The thinner hydrogel films are being used in sensing systems.^{17–19} Hydrogels deposited on solid surfaces, such as titanium, stainless steel, silicon, gold (Au), could enhance their application as polymer-coated implants or controlled release devices (e.g., a stents or a microchip) in the areas of drug delivery and tissue engineering.²⁰ Metal surfaces with patterned chemical functionalities have been produced through vapor deposition of a PHEMA grid resulting in selective cell attachment onto metal and PHEMA substrates.²¹

In a previous work, we successfully electro-synthesized thin films of different poly (acrylic acid) hydrogels onto Ti and Ti-6Al-4V substrates through an electro-reductive process, highlighting possible applications related to corrosion protection or development of bioactive films for titanium-based orthopedic prostheses.^{22–24} In this study, a simple, one-step and organic solvent-free electro-synthetic coating mechanism was investigated to produce uniform and highly adherent PHEMA-based thin films for a wide range of metal substrate. PHEMA and PHEMA–EGDMA were electro-synthesized for the first time on Au substrates, with potential application in biosensors for biomedicine and pharmaceutical screening. Quartz crystal microbalance with dissipation monitoring (QCM-D) was employed to investigate the correlation between the swelling behavior and the thickness of the films. Surface chemistry, wettability, and topography were assessed by X-ray photoelectron spectroscopy (XPS), static contact angle (SCA), and atomic force microscopy (AFM). Cell adhesion assays were carried out using human dermal fibroblasts to evaluate the potential application of PHEMA films as coatings for biomedical applications.

Experimental

Materials

2-Hydroxyethyl methacrylate (HEMA) monomer (Fluka), ethylene glycol dimethacrylate (EGDMA) crosslinker (Fluka), $(\text{NH}_4)_2\text{S}_2\text{O}_8$ (Aldrich), and other chemicals were used as supplied without further purification. AT-cut quartz crystals with Au electrodes (Q-Sense) were used as working electrodes for the electro-polymerization process.

Coating electro-synthesis

The electrochemical experiments were carried out using a PAR 273 potentiostat–galvanostat (EG&G Princeton Applied Research) as reported in previous works.^{23,24} Cathodic and anodic compartments were connected through a glass frit of medium porosity. PHEMA and PHEMA–EGDMA samples were obtained on Au/quartz crystals working electrodes dipped into the cathodic side cell compartment, while a platinum wire was used as counter electrode and was fixed in the anode. The Ag/AgCl, KCl sat. (saturated KCl) reference electrode was positioned in close proximity to the working electrode using a Luggin's capillary. In this study, all potentials refer to the reference system used, Ag/AgCl, KCl sat. 0.197 V versus saturated calomel electrode (SCE).

The electro-polymerizations were carried out in the previously described cell using the following procedure: the cathodic compartment was filled with 0.1 M $(\text{NH}_4)_2\text{S}_2\text{O}_8$ electrolyte solution containing monomer (HEMA) 0.1 M or (HEMA) 0.1 M with crosslinker (EGDMA) (2%, mol/mol), while the anolyte was 0.025 M H_2SO_4 . The catholyte was purged with nitrogen for 10 min before any electro-polymerization. During the electro-synthesis, carried out at room temperature, nitrogen purged the air above the catholyte. At the end of electro-polymerization, the working electrode was removed immediately, washed with distilled water, and then dried in an oven at 50°C. To obtain hydrogel coatings on the Au electrode of the quartz crystal microbalance, this face was used as working electrode. Therefore, it was necessary to employ an appropriate crystal holder to avoid the polymer deposition on the bottom face of the crystal.

Optimal electrochemical conditions, necessary to obtain uniform hydrogel coatings on Au electrodes, were determined by carrying out a series of electro-polymerizations by cyclic voltammetry applying different number of cycles. In particular, the potential was varied from 0.0 to -1.2 V for a number of cycles ranging from 5 to 50 (scan rate = 100 mV/s).

Material characterization

XPS analysis. XPS spectra were obtained with a ThermoVG Thetaprobe spectrometer (Thermo Fisher Scientific, Inc., Waltham, MA, USA) equipped with a microspot monochromatized Al-K α source. The Al-K α line (1486.6 eV) was used throughout; the base pressure was 10^{-9} mbar. Survey scans (binding energy range 0–1200 eV, FAT mode, pass energy = 150 eV) were recorded. Data were analyzed using the Advantage software package. Quantification was done by peak area; comparison of data from different elements was performed by correction with empirically derived atomic sensitivity factors.

AFM characterization. Surface morphology was investigated using AFM measurements performed in an intermittent mode (IC-AFM) using an AutoProbe CP Thermomicroscope. A sharp conical tip with a curvature radius <10 nm and an amplitude of vibration of 80 kHz (dLever Series Probe) mounted on a p-type doped Si cantilever was used. The effect of the number of cycles (20, 30, 40, and 50) and EGDMA addition on the coating morphology (i.e., roughness measurement system, RMS) was investigated.

SCA measurements. These measurements were performed at room temperature in air using manual goniometer (Kernco Instruments Co. Inc.) and applying the sessile drop method. Liquid drops of 5 μL were applied upon the material surface. SCA (θ_s)

measurements for the determination of the hydrophilic/hydrophobic characteristics were estimated by the two-dimensional projection of the droplet on both left and right sides. For PHEMA and PHEMA–EGDMA electro-synthesized hydrogels, pure deionized water (surface free energy $\gamma_w = 72.8 \text{ mJ/m}^2$) was employed as test liquid. Five different measurements were performed on different areas of the same sample. The mean and standard deviation values were recorded for each measurement.

QCM-D measurements. The QCM-D (D300, Q-Sense AB, Göteborg, Sweden) technique was employed to measure the frequency and dissipation shifts, i.e., ΔF and ΔD , by periodically switching off the driving circuit and recording the decay of the damped oscillation. During the measurements, the crystal was mounted in a thermostated liquid chamber, designed to provide a rapid, non-perturbing exchange of the liquid in contact with one side of the sensor. In this study, the frequency and dissipation responses were recorded using the fundamental resonance frequency (around 5 MHz) and the third, fifth, and seventh overtones at 15, 25, and 35 MHz, respectively. For clarity, the results are referred only to the third overtone, normalized to that of the fundamental mode by dividing the frequency data by the overtone number (graphs F3/3 and D3 values were reported). The crystals were cleaned by immersing them in a solution of $\text{H}_2\text{O}_2:\text{NH}_3:\text{H}_2\text{O}$ at 1:1:5 for 5 min at 75°C , and then placed into a UV/ozone chamber for 10 min in a UV/ozone chamber.

The film mass was measured by weighing the dry film in air, at a constant temperature of $37.0 \pm 0.1^\circ\text{C}$, in triplicate. The film density, obtained by a preliminary AFM thickness estimation of pre-weighed coating samples of each polymer, was calculated to be equal to 1.1 and 1.8 g/cm^3 for PHEMA and PHEMA–EGDMA, respectively. The water content percentage (WC%) was evaluated using the following equation:

$$\text{WC} = (W_s - W_d)/W_s \times 100 \quad (1)$$

where W_s and W_d correspond to the weight of swollen and dry hydrogel coatings, respectively. These weights were evaluated by measuring the frequency shifts (i.e., the mass of wet or dry polymer deposited on AT-cut crystals with Au electrodes), in air and in deionized water, respectively, using the Sauerbrey equation.²⁵

As reported in literature,²⁶ the Sauerbrey equation can be considered reliable when the frequency shifts during the experiment are nearly independent of the frequency monitored (i.e., the fundamental and the three overtones), with a maximum dissipation change of $\sim 5 \times 10^{-6}$.

Cell behavior assessment

Human dermal fibroblasts were obtained from skin fragments of three subjects (mean age 31 ± 4) submitted to a surgical treatment of femoral fractures. All subjects gave their informed consent. Tissue fragments were rinsed three times with phosphate-buffered saline and incubated in Dulbecco's modified essential medium (DMEM) containing 1% penicillin-streptomycin, 10% fetal bovine serum (FBS) (all from Sigma–Aldrich, Milan, Italy) in Petri dishes with 60 mm in diameter (Falcon®, Becton Dickinson Labware, NJ, USA). The cells were grown in controlled atmosphere (5% CO_2 ; $T = 37^\circ\text{C}$). The medium was changed twice a week. Confluent cells were detached with 0.25% trypsin in 1 mM EDTA (Sigma–Aldrich) and split 1:2.

Three replicas of each sample (PHEMA and PHEMA–EGDMA) were placed into 24-well polystyrene culture plates. Before cell seeding, specimens were UV-sterilized (wave length of 254 nm) for 48 h (24 h per sheet side) and then seeded with 1.5×10^4 cells suspended in 200 μL of DMEM-FBS and incubated (5% CO_2 , $T = 37^\circ\text{C}$) without any additional medium for 30 min. Afterwards, 2 mL of DMEM-FBS was added to each well. In the control cultures, the cells were placed directly into 24-well polystyrene culture plates (TCPs) at the same density as the other samples. All the samples were cultured for 2 and 7 days.

For SEM analysis, specimens were fixed in 2% glutaraldehyde in 0.1 M cacodylate buffer (pH 7.4), post-fixed in 1% osmium tetroxide, dehydrated in increasing ethanol concentrations, dried in a critical point drier, mounted on aluminum stubs and Au-sputtered. Specimens were observed with a SEM Philips XL 20 (FEI Italia SRL, Milan, Italy).

Results and discussion

The electro-synthesis of linear and crosslinked PHEMA hydrogel coatings from aqueous solution was carried out on Au electrodes. The cyclic voltammograms recorded for PHEMA and PHEMA–EGDMA electro-synthesis on Au electrodes are illustrated in Figure 1. The two reduction peaks in the cyclic voltammograms at -0.95 and -0.55 V (vs. Ag/AgCl reference electrode) were ascribable to H^+ and $\text{S}_2\text{O}_8^{2-}$ ions, respectively. This electro-synthetic route yielded thin, adherent films, on the Au electrodes with good adhesion. Touching the films with tweezers did not leave any marks and no detachments were observed during the swelling experiments while stored in water for weeks.

The polymerization mechanism of acrylic monomers on stainless steel using the same initiator, revealed that the peak reduction currents of H^+ and $\text{S}_2\text{O}_8^{2-}$ were detected at -1.2 and -0.7 V (vs. Ag/AgCl reference electrode), respectively.²⁷ Moreover, when a titanium substrate was used as the working electrode, a single reduction peak at -1.4 V, ascribable to $\text{S}_2\text{O}_8^{2-}$ was detected, as no peak reduction current relevant to H^+ ions was observed in the potential range investigated (0/ -1.6 V).²⁸

The current did not decrease on successive scans for PHEMA (Figure 1(a)), due to the formation of a porous layer on the Au electrode, as confirmed by AFM and SEM. A similar result was observed on titanium substrates.²⁹ On the other hand, a large decrease in the peak current, at the 50th cycle for PHEMA–EGDMA crosslinked system (Figure 1(b)), indicated the formation of a passive coating on the electrode. This behavior is related to a more compact crosslinked hydrogel structure with respect to the uncrosslinked ones. The crosslinking, which hinders the mobility of the polymer chains, made access to the electrode surface more difficult.

XPS analysis was performed on PHEMA and PHEMA–EGDMA hydrogel coatings deposited on Au electrodes by electro-synthesis. Different numbers of cycles (5–50 cycles) were investigated to ascertain the uniform coverage of the Au substrate. For both the crosslinked and uncrosslinked polymers, the wide-scan spectra had C and O signals, related to polymer matrix. An Au signal was detected for films obtained with 5 cycles, whereas no substrate signal was observed when the number of voltammetric cycles was greater than 20.

Wide-scan spectra, relevant to PHEMA coatings, obtained by cyclic voltammetry using 5 and 20 cycles, respectively, are reported in Figure 2. In Figure 3, typical C1s spectra of PHEMA and PHEMA–EGDMA coatings are shown, as well as components obtained from curve fitting. The attributions and binding energy values are reported in Table 1.

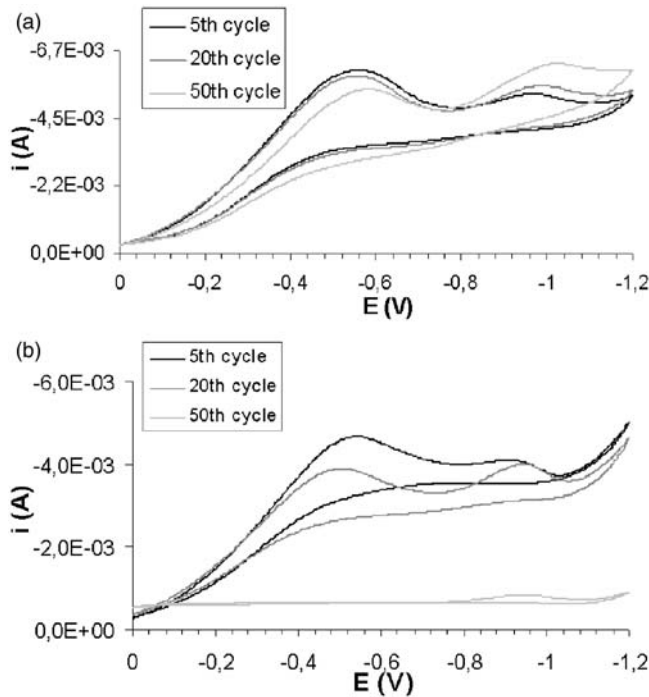


Figure 1. Cyclic voltammograms recorded for the electro-synthesis of PHEMA (a) and PHEMA-EGDMA (b) coatings on Au electrodes.

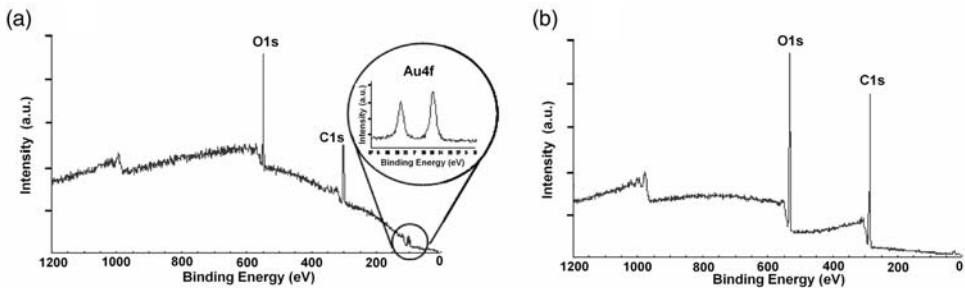


Figure 2. Wide-scan spectra of 5 cycles (a) and 20 cycles (b) of PHEMA coatings on Au electrodes. Note: In the circular inset, the high-resolution spectrum of Au4f region was reported.

C1s signals of PHEMA electro-polymerized on the Au substrate (Figure 3(a)) were fitted by five components. The corrected peak area ratios were very similar to the expected stoichiometry (2:1:1:1:1), which is in agreement with data obtained for PHEMA coatings electro-synthesized on titanium substrates.²³ The C1s curve fitting of PHEMA-EGDMA polymer has been employed to evaluate the amount of EGDMA in the crosslinked polymer electro-synthesized on Au (Figure 3(b)). In particular, the EGDMA incorporation in the

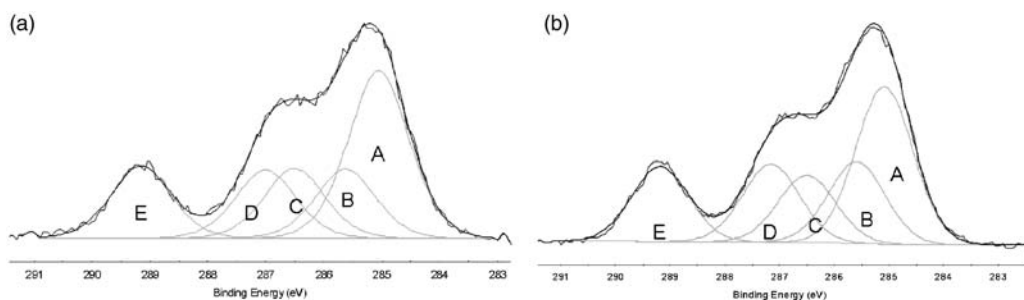


Figure 3. Typical C1s XPS signals recorded on PHEMA (a) PHEMA–EGDMA coatings (b), obtained using 20 voltammetric cycles on Au.

Note: The components and resultants obtained from curve fitting are also shown. Attributions, binding energy values, and atomic percentages were reported in Table 1.

Table 1. Attributions, binding energy values and atomic percentages of XPS C1s signals fitting components relevant to PHEMA and PHEMA–EGDMA coatings on Au substrate.

Attribution	BE (eV)	At.%		
		PHEMA	PHEMA–EGDMA	
A	–CH _x	285.0	37 ± 2	37 ± 2
B	–CC(=O)OR	285.7	16.5 ± 1.5	19.2 ± 1.7
C	–COH	286.5	16.5 ± 1.6	12.8 ± 1.2
D	–COC=O	287.1	15 ± 2	17 ± 2
E	–C(=O)O	289.2	16.0 ± 0.8	14.0 ± 0.5

polymer produced an increase in all the peaks except peak C – relevant to the PHEMA COH functionality – as clearly noticeable by comparing Figure 3(a) and (b). This was relevant to an increment of the (peak E/peak C) areas ratio with respect to that obtained for the uncrosslinked system. This increment allowed estimate a surface EGDMA percentage equal to $(9 \pm 2)\%$ (data calculated over at least three replicates).

By comparing this value with the nominal amount of EGDMA employed in the electrosynthesis (2%), it was concluded that a surface enrichment in the crosslinker on the electro-synthesized system occurred. No significant statistical differences have been observed by varying the number of voltammetric cycles, denoting that this parameter did not affect the surface chemical composition of the electro-synthesized materials.

The AFM investigations showed the influence of the hydrogel type and number of cycles on the coating surface roughness (RMS) (Figure 4(a)). Increasing the number of cycles from 20 to 50, the RMS of PHEMA hydrogels decreased from 8.5 to 2.3 nm. The addition of the crosslinker strongly affected the morphological organization of the hydrogel, resulting in a smoother surface. For example, at 50 cycles, with the crosslinker, the RMS decreased from 2.3 to 1.5 nm.

Three-dimensional $1 \times 1 \mu\text{m}^2$ topographical images of PHEMA and PHEMA–EGDMA coatings electro-synthesized with 20 and 50 cycles are shown in Figure 4(b)–(e). Their

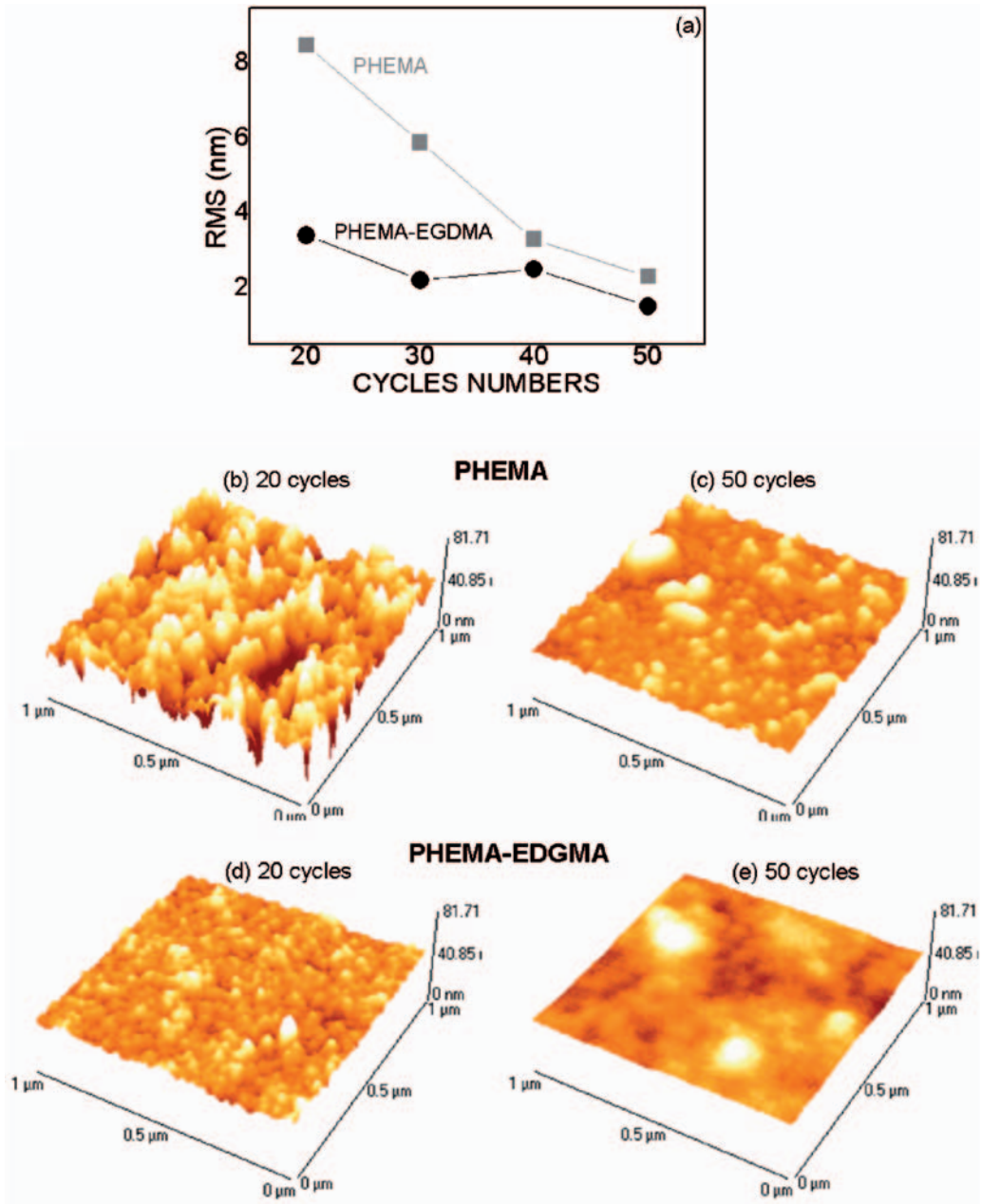


Figure 4. (a) Coatings roughness (RMS) dependence on the cycle numbers and the hydrogel type. Notes: Three-dimensional topographical images of PHEMA coatings electro-synthesized by 20 (b) and 50 (c) cycles and PHEMA-EGDMA coatings electro-synthesized by 20 (d) and 50 (e) cycles are also shown. The vertical scale for all AFM images is 0–81.71 nm.

morphology appears as a granular structure with grain densities and RMS that decreased with the number of cycles and/or the addition of the crosslinking agent. Therefore, from a morphological point of view, the addition of EGDMA to PHEMA-based hydrogels yields more uniform coatings on Au surfaces.

SCA were used to determine the surface hydrophilicity (or wettability) of PHEMA-based electro-synthesized coatings. The contact angles and photographs of water drops on 20 cycles of electro-synthesized PHEMA and PHEMA–EGDMA coatings are reported in Figure 5. The relevant contact angle values are expressed as mean \pm standard deviation on at least five measurements. PHEMA contact angle value resulted equal to $61 \pm 5^\circ$, while for PHEMA–EGDMA the value was found to be slightly higher and equal to $67 \pm 4^\circ$, regardless of the number of cycles employed during the coating electro-synthesis process. This could be attributed to a homogeneous covering of the Au substrate in all the experimental conditions adopted for the polymer synthesis, independently of their very low thickness when produced by a lower number of cycles. The addition of crosslinker did not significantly alter the hydrophilicity of the PHEMA system, as observed by performing the statistical *t*-test on the mean values of the two groups ($\alpha = 0.05$).

By comparing our data with the literature, the electro-synthesized PHEMA thin hydrogel coating resulted slightly more hydrophobic than a membrane obtained by UV

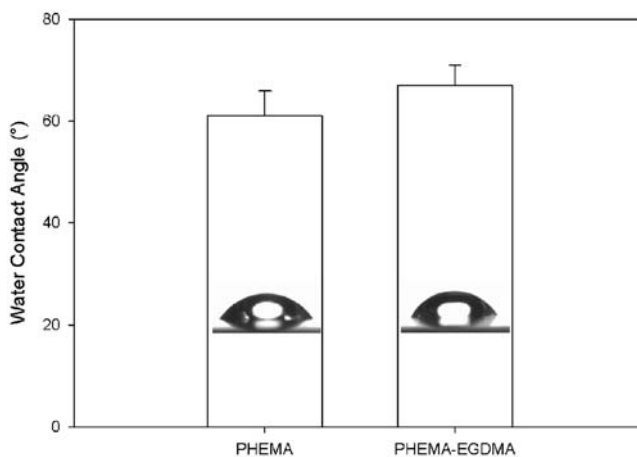


Figure 5. Water contact angles on 20 cycles of PHEMA and PHEMA–EGDMA.

Table 2. Film thickness and water content percentage as a function of the number of voltammetric cycles employed in the synthesis of PHEMA and PHEMA–EGDMA coatings.

Number of cycles	PHEMA		PHEMA–EGDMA	
	Thickness (nm)	WC%	Thickness (nm)	WC%
5	8 ± 1	81 ± 3	5 ± 2	75 ± 3
20	34 ± 4	69 ± 3	20 ± 5	61 ± 3
50	84 ± 9	60 ± 2	51 ± 8	53 ± 5

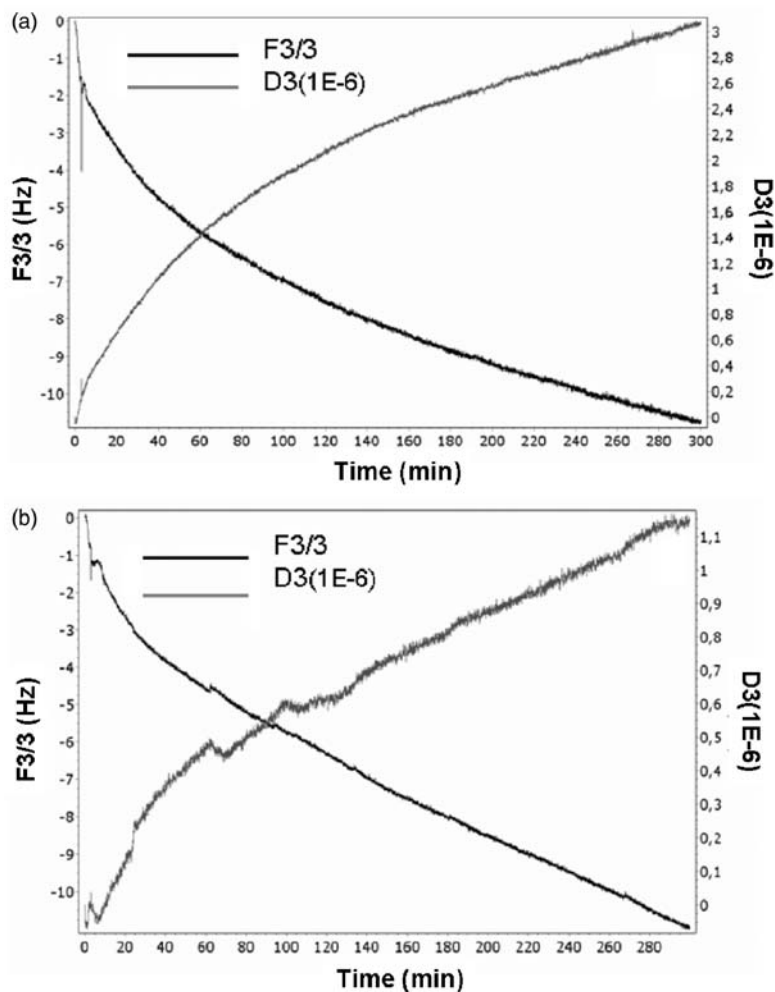


Figure 6. QCM-D monitoring of 20 cycles of PHEMA (a) and 20 cycles of PHEMA-EGDMA (b) swelling process in water.

photopolymerization, where contact angle values were $55.6 \pm 1.4^\circ$.³⁰ It is important to underline that SCA measurements represent only an image of the polymer-water interaction, thus not the possible rearrangements, water uptake and conformational changes of the polymer after the contact with aqueous medium. By monitoring the evolution of water-polymer interaction over a non-instantaneous time period using QCM-D, important differences in terms of film thickness and swelling properties can become appreciable.

The high sensitivity of QCM-D enables investigation of the swelling kinetics, hydration states, and viscoelastic changes in macromolecules such as proteins, polymers.^{31,32} In this study, QCM-D was used to evaluate the film thickness, by varying the number of voltammetric cycles in air, at 37°C (Table 2). For both PHEMA and PHEMA-EGDMA

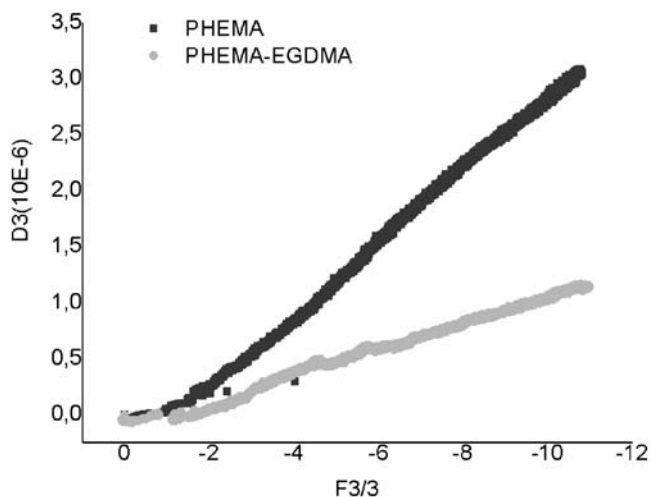


Figure 7. DF-plots relevant to the PHEMA and PHEMA–EGDMA swelling processes reported in Figure 6.

coatings, regardless the number of cycles employed, reduction in terms of film thickness was obtained by adding the crosslinker.

By applying 5 cycles, extremely thin coatings were obtained, thus allowing us to ascribe the presence of Au signal in the XP spectrum (Figure 2(a)) to the extremely thin film coatings (<10 nm) (Table 2). In the presence of the crosslinker, a reduction in film thickness was seen for all the voltammetric cycles. For example, 50 cycles of PHEMA–EGDMA coatings are in good agreement with the total current decrease in the cyclic voltammogram (Figure 1(b)).

The swelling kinetics of 20 cycles of PHEMA and PHEMA–EGDMA hydrogel films are shown in Figure 6(a) and (b), respectively. The frequency and dissipation were simultaneously detected for 5 hours, to analyze possible modifications of the polymer viscoelastic properties during absorption of water, before reaching its equilibrium hydration level. The ΔF values are affected by both the change in viscosity from air to aqueous solution and by the adsorbed water in the films. Therefore, the water uptake values were corrected to take into account this bulk effect (viscosity).³³ Based on the frequency shifts (Figure 6), the PHEMA and PHEMA–EGDMA coatings had similar water uptake.

The differences between the swelling kinetics of the uncrosslinked and crosslinked PHEMA coating are depicted in the DF-plot (Figure 7). The DF slope for PHEMA was higher than for PHEMA–EGDMA, due to the presence of the crosslinker in the latter which hampers the chain mobility and relaxation parameters (as well as the dissipation factor, monitored by QCM-D). Therefore, even though PHEMA and PHEMA–EGDMA films displayed similar water uptake, different kinetics of conformational relaxation of polymer chains were seen.

The WC% decreased with increasing film thickness (Table 2) which may be due a densification of the film during the electro-polymerization making it less prone to swelling.³⁴ For all of the voltammetric cycles, the WC% of the resultant coatings was influenced by the crosslinker. This is in agreement with previous WC% results for PHEMA and PHEMA crosslinked with 2% ethylene glycol diacrylate films, electro-synthesized on Ti sheets that gave 69 and 52 WC%, respectively.²³

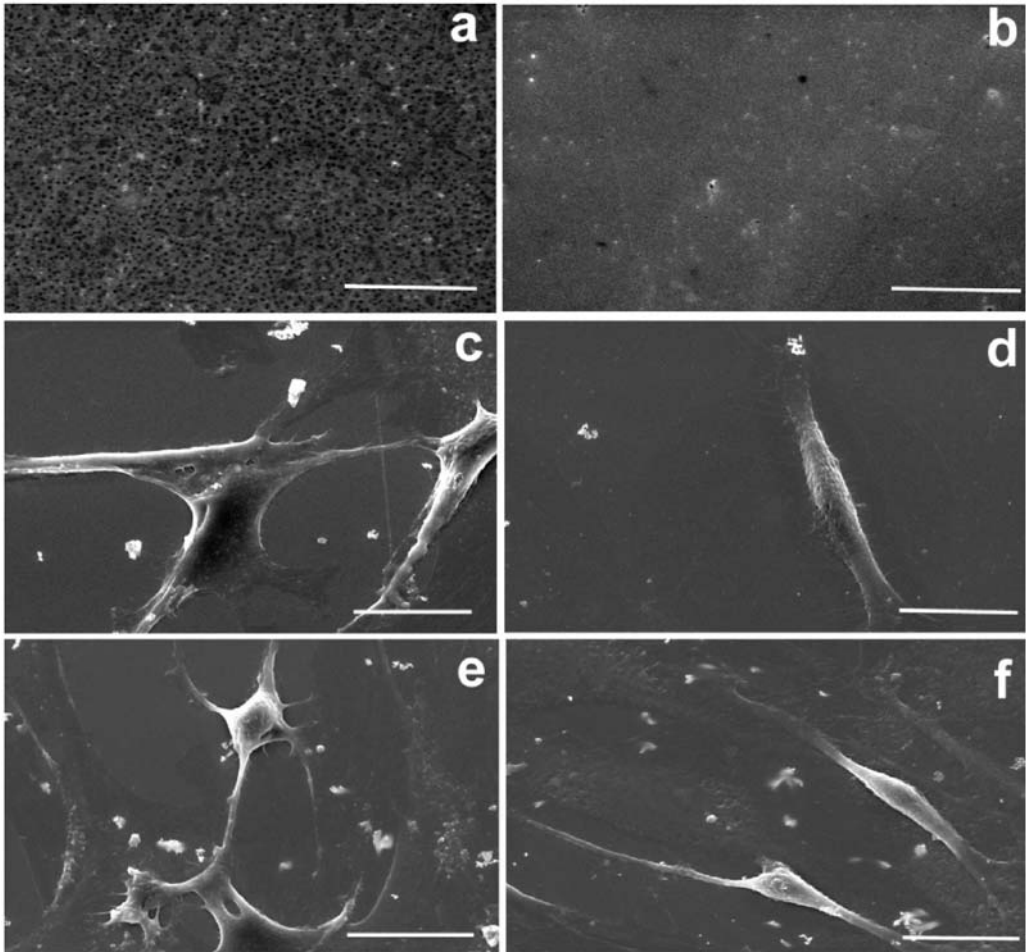


Figure 8. SEM micrographs of PHEMA (a) and PHEMA–EGDMA (b) hydrogels showing the different porosities of the two coatings. Fibroblasts cultured on PHEMA after 2 (c) and 7 days (e) displayed a spread morphology, while cells cultured on PHEMA–EGDMA coatings after 2 (d) and 7 days (f) were more elongated in shape. Scale bar 20 μm .

The water uptake for PHEMA and PHEMA–EGDMA disks or cylinders had significantly lower WC% values and slower swelling kinetics than our systems.¹⁴ The large deviation could be due to the fact that the hydrogels in this study were electro-polymerized in aqueous solution and consequently resulted more porous. When the polymers are electro-polymerized onto metal substrates, the polymer density, crosslinking degree, and flexibility of the chains bound to the solid substrate could significantly differ from the bulk materials.

Cell behavior

We previously used MG-63 human osteoblast-like cells to investigate osteoblast behavior on electro-synthesized PHEMA-based coatings.²⁹ Since most polymers are considered to be a

poor substratum for cell adhesion and proliferation, the spreading data for PHEMA was in contrast with the literature;^{35–37} in this case, the cell adhesion was determined by the topography of the underlying titanium substrate.^{38,39} In this study, the surface morphologies obtained arose from the polymer structure with a metal substrate (i.e., Au electrodes). Therefore, the cell behavior can be ascribable directly to PHEMA and PHEMA–EGDMA coating features. The two different coatings PHEMA and PHEMA–EGDMA gave different porosities, good fibroblast adhesion and growth onto the two different thin hydrogel coatings was observed in Figure 8(a) and (b), after 2 days (Figure 8(c) and (d)) and 7 days (Figure 8(e) and (f)) of culture. This is in contrast with literature that reports poor fibroblast adhesion to pure PHEMA.⁴⁰

Although very thin, the PHEMA and PHEMA–EGDMA coatings electro-polymerized on the Au substrates were able to sustain primary fibroblast adhesion and growth, differences in cell morphology and/or spreading between the two tested polymers. The PHEMA coating gave a sponge-like surface that enhanced cell attachment and spreading while the more compact and smooth PHEMA–EGDMA coatings cells tended to have a more elongated shape. This could be related to the different porosity and roughness of the two polymeric substrates. The electro-synthesis of PHEMA-based coatings on Au substrates presents an interesting platform for biosensing applications, enabling different surface topographies to be made by simply varying the number of cycles for the polymer growth and being crosslinked or not.

Conclusions

PHEMA and PHEMA–EGDMA hydrogel thin films have been successfully electro-synthesized on Au electrodes and characterized. In particular, QCM-D analysis confirmed the relationships between: (1) the number of voltammetric cycles and the film thickness; (2) the film thickness and the water uptake; and (3) the presence of the crosslinker and the conformational relaxation of the polymer chains. The morphological of the fibroblast culture examined by SEM confirmed that a hydrogel surface has a strong effect on cell adhesion. It is proposed that these systems could be successfully exploited both in biomedical and diagnostic devices.

Acknowledgements

The authors thank Prof. P. Cosma of Bari University for useful discussions about electrochemical measurements. We also thank to Mr G. Cosmai for the fabrication of the crystal holder and Mr S. Giacommo, Dr A. Pedico, and Dr C. Ferretti for their technical assistance. This study was partly supported by grants to Dr De Giglio (National grant Progetto Strategico cod. CIP PS_046 ‘Studio e Sviluppo di Materiali Innovativi per Applicazioni in Chirurgia Laser della Cornea’ founded by the Apulia Region) and Dr Mattioli-Belmonte (RSA 2009, Marche Polytechnic University).

References

1. Peppas NA, Hilt JZ, Khademhosseini A and Langer R. Hydrogels in biology and medicine: from fundamentals to bionanotechnology. *Adv Mater* 2006; 18: 1345–1360.
2. Bruck SD. Aspects of three types of hydrogels for biomaterial applications. *J Biomed Mater Res* 1973; 7: 387–404.

3. Brazel CS and Peppas NA. Dimensionless analysis of swelling of hydrophilic glassy polymers with subsequent drug release from relaxing structures. *Biomaterials* 1999; 20: 721–732.
4. Lu S and Anseth K. Photopolymerization of multilaminated poly(HEMA) hydrogels for controlled release. *J Control Release* 1999; 57: 291–300.
5. Zahedi P and Lee PI. Solid molecular dispersions of poorly water-soluble drugs in poly(2-hydroxyethyl methacrylate) hydrogels. *Eur J Pharm Biopharm* 2007; 65: 320–328.
6. Kliment K, Stol M, Fahoun K and Stockar B. Use of spongy hydron in plastic surgery. *J Biomed Mater Res* 1968; 2: 237–243.
7. Nathan P, Macmillan BG and Holder IA. Effect of a synthetic dressing formed on a burn wound in rats: a comparison of allografts, collagen sheets and polyhydroxyethylmethacrylate in the control of wound infection. *Appl Microbiol* 1974; 28: 465–468.
8. Wichterle O and Lim D. Hydrophilic gels for biological use. *Nature* 1960; 185: 117–118.
9. Katime I and Rodríguez E. Absorption of metal ions and swelling properties of poly(acrylic acid-co-itaconic acid) hydrogels. *J Macromol Sci Pure Appl Chem A* 2001; 38: 543–558.
10. Bartolo PJ, Chua CK, Almeida HA, Chou SM and Lim ASC. Biomufacturing for tissue engineering: present and future trends. *Virtual Phys Prototyping* 2010; 4(4): 203–216.
11. Bartolo PJ. Multimaterial microstereo-termitografia (microSTLg). *Research project financed by the Portuguese Foundation for Science and Technology (FCT)* 2008.
12. Davis TP and Huglin MB. Effect of crosslinking on the properties of poly(2-hydroxyethyl methacrylate) hydrogels. *Angew Makromol Chem* 1991; 189: 195–205.
13. García O, Blanco MD, Gómez C and Teijón JM. Effect of the crosslinking with 1,1,1-trimethylolpropane trimethacrylate on 5-fluorouracil release from poly(2-hydroxyethyl methacrylate) hydrogels. *Polym Bull* 1997; 38: 55–62.
14. Mabilieu G, Stancu IC, Honoré T, Legeay G, Cincu C, Baslé MF, et al. Effects of the length of crosslink chain on poly(2-hydroxyethyl methacrylate) (pHEMA) swelling and biomechanical properties. *J Biomed Mater Res A* 2006; 77(1): 35–42.
15. Allen PEM, Bennett DJ and Williams DRG. Water in methacrylates—I. Sorption and desorption properties of poly(2-hydroxyethyl methacrylate-co-glycol dimethacrylate) networks. *Eur Polym J* 1992; 28: 347–352.
16. Feller JF, Guezenoc H, Bellegou H and Grohens Y. Smart poly(styrene)/carbon black conductive polymer composites films for styrene vapour sensing. *Macromol Symp* 2005; 222: 273–280.
17. Blanco-López MC, Gutiérrez-Fernández S, Lobo-Castañón MJ, Miranda-Ordieres AJ and Tuñón-Blanco P. Electrochemical sensing with electrodes modified with molecularly imprinted polymer films. *Anal Bioanal Chem* 2004; 378: 1922–1928.
18. Herlem G, Lakard B, Herlem M and Fahys BJ. pH sensing at Pt electrode surfaces coated with linear polyethylenimine from anodic polymerization of ethylenediamine. *Electrochem Soc* 2001; 148: E435–E438.
19. Kikuchi A and Okano T. Nanostructured designs of biomedical materials: applications of cell sheet engineering to functional regenerative tissues and organs. *J. Controlled Release* 2005; 101: 69–84.
20. Buchhold R, Nakladal A, Gerlach G, Herold M, Gauglitz G, Sahre K, et al. Swelling behavior of thin anisotropic polymer layers. *Thin Solid Films* 1999; 350: 178–185.
21. O’Neill C, Jordan P and Riddle P. Evidence for two distinct mechanisms of anchorage stimulation in freshly explanted and 3T3 swiss mouse fibroblasts. *J Cell Sci* 1990; 95: 577–586.
22. De Giglio E, Cometa S, Cioffi N, Torsi L and Sabbatini L. Analytical investigations of poly(acrylic acid) coatings electrodeposited on titanium-based implants: a versatile approach to biocompatibility enhancement. *Anal Bioanal Chem* 2007; 389: 2055–2063.
23. De Giglio E, Cometa S, Satriano C, Sabbatini L and Zamboni PG. Electrosynthesis of hydrogel films on metal substrates for the development of coatings with tunable drug delivery performances. *J Biomed Mater Res A* 2009; 88(4): 1048–1057.
24. De Giglio E, Cafagna D, Ricci MA, Sabbatini L, Cometa S, Ferretti C and Mattioli-Belmonte M. Biocompatibility of poly(Acrylic Acid) thin coatings electro-synthesized onto TiAlV-based implants. *J Bioact Compat Polym* 2010; 25: 374–391.
25. Sauerbrey G. The use of quartz oscillators for weighing thin layers and for microweighing. *Z Phys* 1959; 155: 206–212.
26. Vogt BD, Lin EK, Wu W and White CC. Effect of film thickness on the validity of the Sauerbrey equation for hydrated polyelectrolyte films. *J Phys Chem B* 2004; 108: 12685–12690.

27. Cram SL, Sprinks GM, Wallace GG and Brown HR. Mechanism of electropolymerisation of methyl methacrylate and glycidylacrylate on stainless steel. *Electrochim Acta* 2002; 47: 1935–1948.
28. De Giglio E, Cometa S, Spoto G, Sabbatini L and Zamboni PG. Electrosynthesis and analytical characterization of PMMA coatings on titanium substrates as barriers against ion release. *Anal Bioanal Chem* 2005; 381: 626–633.
29. De Giglio E, Cometa S, Ricci MA, Zizzi A, Cafagna D, Manzotti S, et al. Development and characterization of rhVEGF-loaded poly(HEMA–MOEP) coatings electrosynthesized on titanium to enhance bone mineralization and angiogenesis. *Acta Biomater* 2010; 6: 282–290.
30. Arca MY, Yılmaz M, Yalçın E and Bayramoğlu G. Surface properties of reactive yellow 2 immobilised pHEMA and HEMA/chitosan membranes: characterisation of their selectivity to different proteins. *J Membrane Sci* 2004; 240: 167–178.
31. Hook F, Kasemo B, Nylander T, Fant C, Sott K and Elwing H. Variations in coupled water, viscoelastic properties, and film thickness of a Mefp-1 protein film during adsorption and cross-linking: a quartz crystal microbalance with dissipation monitoring, ellipsometry, and surface plasmon resonance study. *Anal Chem* 2001; 73(24): 5796–5804.
32. Wang ZH, Kuckling D and Johannsmann D. Temperature-induced swelling and de-swelling of thin poly(*N*-isopropylacrylamide) gels in water: combined acoustic and optical measurements. *Soft Mater* 2003; 1(3): 353–364.
33. Aulin C, Ahola S, Josefsson P, Nishino T, Hirose Y, Osterberg M and Wagberg L. Nanoscale cellulose films with different crystallinities and mesostructures—their surface properties and interaction with water. *Langmuir* 2009; 25: 7675–7685.
34. Reuber J, Reinhardt H and Johannsmann D. Formation of surface-attached responsive gel layers via electrochemically induced free-radical polymerization. *Langmuir* 2006; 22: 3362–3367.
35. Lydon MJ, Minnet TV and Tighe BJ. Cellular interactions with synthetic polymer surfaces in culture. *Biomaterials* 1985; 6(6): 396–402.
36. Filmon R, Baslé MF, Atmani H and Chappard D. Adherence of osteoblast-like cells on calcospherites developed on a biomaterial combining poly(2-hydroxyethyl) methacrylate and alkaline phosphatase. *Bone* 2002; 30: 152–158.
37. Zhang L, Ramsaywack S, Fenniri H and Webster TJ. Enhanced osteoblast adhesion on self-assembled nanostructured hydrogel scaffolds. *Tissue Eng Part A* 2008; 14: 1353–1364.
38. Deligianni DD, Katsala N, Ladas S, Sotiropoulou D, Amedee J and Missirlis YF. Effect of surface roughness of the titanium alloy Ti–6Al–4V on human bone marrow cell response and on protein adsorption. *Biomaterials* 2001; 22: 1241–1251.
39. Ciardelli G, Gentile P, Chiono V, Mattioli-Belmonte M, Vozzi G, Barbani N, et al. Enzymatically crosslinked porous composite matrices for bone tissue regeneration. *J Mater Res A* 2010; 92: 137–151.
40. Horbett TA, Waldburger JJ, Ratner BD and Hoffman AS. Cell adhesion to a series of hydrophilic-hydrophobic copolymers studied with a spinning disc apparatus. *J Biomed Mater Res* 1988; 22: 383–404.